THE VELOCITY FIELD IN THE NEAR WAKE OF A FREELY-OSCILLATING CIRCULAR CYLINDER AT LOCK-IN

Gregory A. Kopp, Salim Fathi, Brian Havel, Robert J. Martinuzzi and Jon Galsworthy
Boundary Layer Wind Tunnel Laboratory
Faculty of Engineering, University of Western Ontario
London, Ontario, N6A 5B9, Canada

ABSTRACT

Two-component velocity measurements were made with laser Doppler velocimetry in the near wake of a freely vibrating, elastically mounted, light weight circular cylinder at lock-in. Maximum cylinder displacements of 0.75d were observed for a mechanical damping level of about 0.2% of critical. The Scruton number was 1.5, while the Reynolds number at lock-in was about 53,000. The velocity data were phase averaged relative to the periodic loading cycle. Significant differences in the details of the turbulence when the cylinder is oscillating compared to the stationary case were observed. These differences lead to increased production of incoherent turbulence. Interestingly, the wake of the oscillating cylinder is narrower than that for the stationary cylinder, so that less engulfment has occurred in spite of the increased strength of the main vortices. This is attributed to the reduced three-dimensionality during formation, in particular, the mitigation of oblique shedding and vortex dislocations.

INTRODUCTION

Fluid flow around circular cylinders and other bluff bodies have been extensively studied for over 100 years because of the rich fluid dynamic behaviour that can be observed and the important applications such as wind loads, mixing, etc.

Vortex shedding, in particular, is a complex process involving three-dimensional instabilities, even for cylinders of very long aspect ratio. At relatively low Reynolds numbers, several studies have shown two modes of three-dimensional instabilities (Modes A and B) which yield small scale streamwise vortices (Williamson, 1996). In the range $1{,}000 < Re < 200{,}000$ there is transition in the separated shear layers. In this Reynolds number range there are base pressure fluctuations which cause shedding at random oblique angles that are accompanied by dislocations. Dislocations are relatively large scale three-dimensional structures which Tombazis and Bearman (1997) have associated with vortex splitting. This allows the redistribution of vorticity such that vortices of the same sign can connect across cells with the different frequencies associated with oblique shedding (Eisenlohr and Eckelmann, 1989). Figure 1 shows typical spanwise spectra associated with this phenomena (Bailey et al., 2002).

When a cylinder is flexible, it will oscillate when the vortex shedding frequency is close to the natural frequency. This is often modeled in the wind tunnel with a section of cylinder mounted elastically to a spring-damper system. The interesting aspect, which motivated the present study, is that, as the cylinder moves, the vortex shedding process is modified. Figure 2 depicts the spectra of pressure fluctuations along the span for an oscillating cylinder. This figure indicates the shedding has become quite two-dimensional with the oblique shedding significantly mitigated. Details pertaining to other aspects of oscillating cylinders can be found in many references (e.g., Sarpkaya, 1979; Bearman, 1984).

Two modes of vortex shedding are known to exist in the synchronization range: one is a vortex street similar to the Kármán street for the stationary cylinder, while the other has

twice as many vortices in the near wake. Williamson and Roshko (1988) call these the '2S' and '2P' modes, respectively. The '2S' mode forms differently than for a stationary cylinder, with four vortices shed; however, the two like-signed vortices pair in the base region so that by a few diameters downstream the overall appearance of the wake is like that for a stationary cylinder. For the '2P' mode, this early pairing does not occur resulting in twice as many spanwise vortices in the near wake.

The objective of the present work is to observe quantitatively how the wake of an oscillating cylinder in the 2S mode differs from the wake of a stationary cylinder.

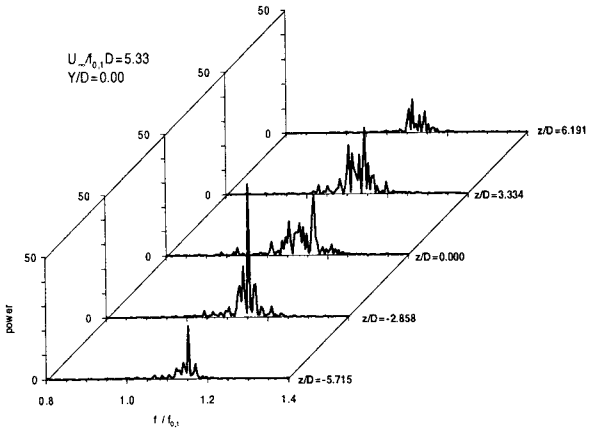

Figure 1. Spectra of pressure fluctuations along the span of the cylinder for a reduced velocity of 5.33 with the cylinder fixed (power spectra are of arbitrary scale).

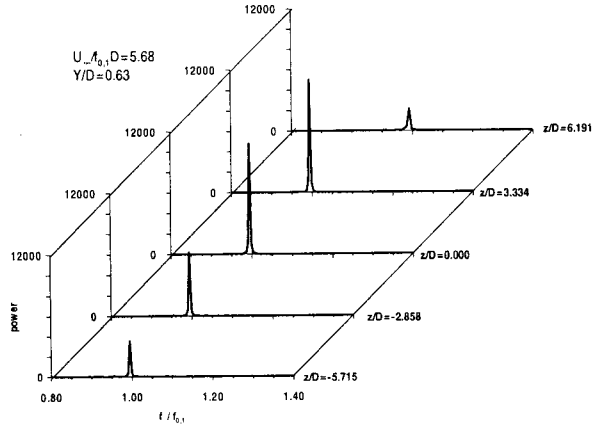

Figure 2. Spectra of pressure fluctuations along the span of the cylinder for a reduced velocity of 5.68 with the cylinder oscillating at maximum amplitude (power spectra are of arbitrary scale).

EXPERIMENTAL DETAILS

All experiments were performed in Boundary Layer Wind Tunnel I at the University of Western Ontario. This tunnel is of the open return type, with a test section 2.4 m wide and of height varying from 1.5 to 2.1 m along the 33 m length. The maximum speed is about 15 m/s and the freestream turbulence is about 1%. A light (~ 1.4 kg), but rigid, carbon-fibre cylinder, L = 2.13 m (7.0 feet) long with a 15.9 cm (6.25 inches) outer diameter, *d*, was constructed. The cylinder was elastically-mounted with eight springs about 3.2 m from the inlet to the test section. Drag lines were attached to allow motions only in the vertical (across wind) direction.

Mechanical damping was measured in-situ in still air. For larger displacements (greater than 0.5d), the damping ratio was estimated to be 0.2% of critical, while at small amplitudes it was 0.05%. No additional mechanical damping was provided. The natural frequency, f_n, of the cylinder-spring system is 5.86 Hz. The mass of the mechanical system is about M = 4.0 kg (about 1/3 of the spring mass is in motion). The Scruton number, $Sc = 2\delta_s M/(\rho d^2 L) = 1.5$, where ρ is the density of air and δ_s is the logarithmic decrement of damping. The total stiffness is 5500 kg/s^2. A photograph of the cylinder and mechanical mounting system can be seen in Figure 3.

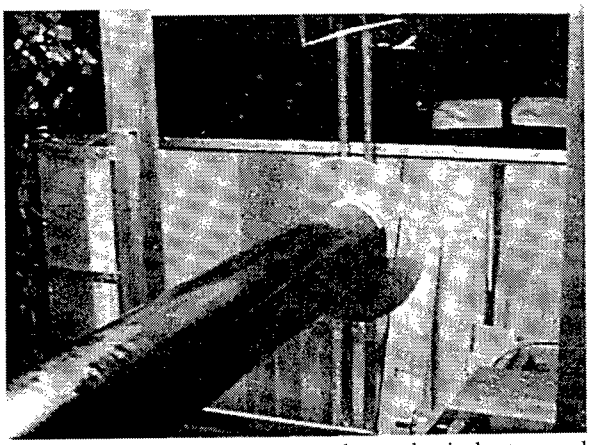

Figure 3. A photograph showing the mechanical set-up and the carbon-fibre cylinder.

The cylinder was designed so that a relatively high Reynolds number and large oscillations could be achieved at lock-in. The Reynolds number, $Re = U_o d/\nu$, at lock-in, was about 53,000 implying a Strouhal number of 0.19 at the maximum amplitude of oscillation. The objective of achieving as high a Reynolds number as possible led to the relatively high blockage ratio of about 8% while the aspect ratio of the cylinder was about 14. No blockage corrections were made to the data. End plates, which can be seen in figure 3, were mounted to the cylinder in order to avoid the effects of the gap which allowed the connection of the cylinder to the mechanical system. The spring system can also be seen through the glass in figure 3 as can the downstream end of the support frame. This frame blocked optical access for a portion of the LDV measurements reported herein. The wind tunnel speed, U_o, was controlled and measured via an upstream Pitot-static tube.

Figure 4 shows the root-mean square (rms.) values of the cylinder displacement versus the reduced velocity, V_r =

$U_o f_n/d$, for an experiment done with an increasing wind tunnel speed. Peak displacements were about 0.63 d at V_r = 5.68 when the pressure tubing system was in place. The velocity measurements reported herein were performed with the tubing system removed. This lowered the mechanical damping and increased the amplitude of the oscillations to 0.75 d.

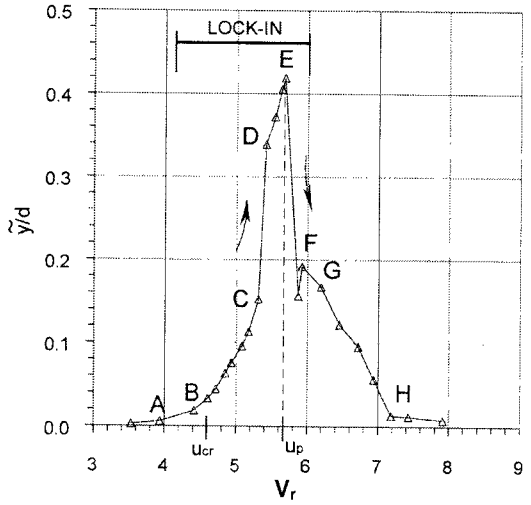

Figure 4. RMS values of the displacement for an increasing wind speed (Fathi, 2001).

The velocity field measurements were obtained with a two-component TSI 9000 series fibre-optic LDV system with a 5 W Ar-Ion light source operated in back-scatter mode. A 2.6x beam expander with a 1520 mm focal length lens were used. The resulting measurement volume was 150 μm and the length was 4.9 mm. For phase-averaging the velocity field, load cell measurements were used as the reference signal. The LDV processor data start-pulse was used to trigger acquisition of the load cell data. The load cell signals were sampled at 200 Hz until the LDV acquired 30,000 points. More than 400 locations in the lower half wake were measured. The load cell reference signal was then processed to determine the cycle. After being low-pass filtered at 1.5 times the shedding frequency, peak detection was performed using a quadratic fit-based algorithm. The filter was a two-pass, phase preserving, numerical filter. Peak-to-peak locations defined the cycle length and the LDV time series were then processed using phase-averaging software where the signals were aligned and the phase decomposition performed. Further details can be found in Havel (1999). The data was distributed in 20, 30 and 40 bins to check convergence. The results using 20 bins are reported herein. Further details regarding the experimental set-up, the resulting data, and the analysis can be found in Fathi (2001) and Kamprath (2001).

PHASE-AVERAGED VELOCITY FIELD

Following the approach of Cantwell and Coles (1983), hereafter referred to as CC83, the upper half wake is plotted from the data in lower half using the fact the motions in the upper and lower halves of the wake are 180° out-of-phase. Additionally, the sign of the lateral velocity component is reversed. The convection velocity, U_c, represents the nominal speed of the vortices so that removing the convection speed from the phase-averaged velocity allows the vortices to be clearly observed. However, determining the appropriate convection speed just downstream of formation is not entirely straightforward. In the range between x/D = 3.5 to 6, there is relatively little change in the convection speed and the value used ($0.68U_o$) represents a good average value in this region. This value is lower than the value found by CC83 of 0.755 U_o at x/d = 3.75 for the wake of a stationary cylinder.

Figure 5 shows the velocity with the cylinder at the uppermost point (y ~ 0.75D) in its cycle of motion. At this location it is observed a vortex has been fully formed from the upper shear layer and is convecting downstream with its centre just beyond x/d = 2 (in the region where no measurements could be taken). The lower shear layer is significantly curved as evidenced by the strong curvature of the sectional streamlines near x/d = 1 and y/d = -0.5. There are also high levels of vorticity in this region. It almost appears as if the flow is moving to fill in the region that the cylinder just vacated as it moves upward. This makes sense when it is considered that the average velocity of the cylinder during one cycle is about $0.56U_o$ so that the instantaneous angle of attack is (relative to an observer attached to the cylinder) about 45° when the cylinder is at its maximum velocity as it passes through the centreline.

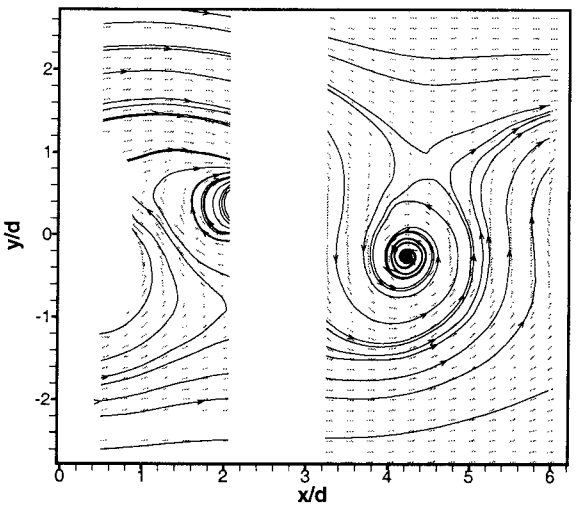

Figure 5. Phase averaged velocity vectors and sectional streamlines using a convection speed, $U_c = 0.68\ U_o$. The cylinder position is at the uppermost location (y = 0.75 D).

As the cylinder moves downwards, the vortex continues to form in the lower shear layer. When the cylinder is located at half of its maximum displacement, the peak (observed) vorticity is found at x/d ~ 1.1 and y/d ~ -0.3 and is $\omega_z/(U_o/d)$ ~ 3. By the time the cylinder reaches the centreline, the lower vortex is fully formed, as shown in Figure 6. The

presence of a saddle point (x/d = 1.2, y/d = 0.6) indicates that fluid from the upper shear layer is curving into the base region, cutting off the lower shear layer so that the fully formed vortex moves downstream and formation of the upper vortex begins. By the time the cylinder reaches its lowermost location, the lower vortex has been convected to about x/d ~ 2.4. This process is similar to that described in Sarpkaya (1979), the flow visualizations by Williamson and Roshko (1988) corresponding to the '2S' mode (see their Figure 10), and the unswitched patterns of Gu et al. (1994) corresponding to f_s/f_n = 1.0 (although there appears to be significant Reynolds number effects. Thus, the present experiments correspond to "normal" vortex shedding.

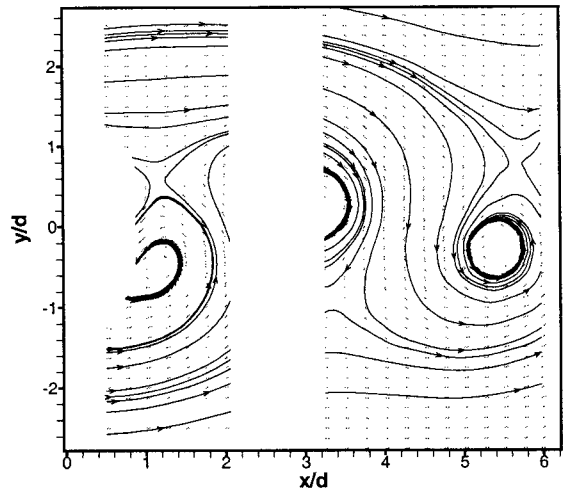

Figure 6. Phase averaged velocity vectors and sectional streamlines using a convection speed, U_c = 0.68 U_o. The cylinder position is at the centreline (y ~ 0.0) and is moving downwards.

VORTICITY AND CIRCULATION

Figure 7 depicts the phase-averaged vorticity, $<\omega_z>/(U_o/d)$ when the cylinder is located on the wake centreline (i.e., the cylinder rest location) and moving downwards. The peak vorticity of the fully formed vortex is about $<\omega_z>/(U_o/d)$ ~ 3.0. By the time the vortices reach x/d ~ 5.4 (bin 11), the peak vorticity has dropped to about 1.6, about 30% larger than that found by CC83 at the same location ($<\omega_z>/(U_o/d)$ ~ 1.2). This is consistent with the observations of Davies (1976; see also Sarpkaya, 1979). However, the nominal size of the vortices is about the same as for the stationary cylinder studied by CC83. Since the base suction coefficient, $-C_{pb}$, increases with oscillation amplitude, both the drag and the initial shed circulation,

$$\frac{\Gamma_o}{U_o d} = \frac{(1 - C_{pb})}{2St}$$

(Roshko, 1954; Bearman and Obasaju, 1982) must be larger than for the stationary cylinder. Our estimate of the circulation in the formed vortices, Γ_v, shows that the ratio, Γ_v/Γ_o, appears to be less than that for stationary cylinders; thus, the shed vortices, though stronger in absolute magnitude, are relatively weaker.

Figure 7 also provides an opportunity to evaluate the approximate spacing ratio, *b/a*, of the fully formed vortex street (where *b* is the vertical spacing between vortices on opposite sides of the wake and *a* is the horizontal spacing between vortices of the same sign). The vertical spacing is observed to be ~0.7d while the horizontal spacing is ~ 4.2d, giving a ratio, *b/a* ~ 0.16. This is, of course, much less than the theoretical value of 0.281 found by von Karman in his linear stability analysis of point vortices, but is suprisingly similar to the value of ~ 0.7/4.3 = 0.16 found by CC83. Thus, the relatively large amplitude motions of the cylinder, do not effect the vortex spacing in the '2S' mode (although, as will be shown later, they will affect other aspects of vortex formation and development).

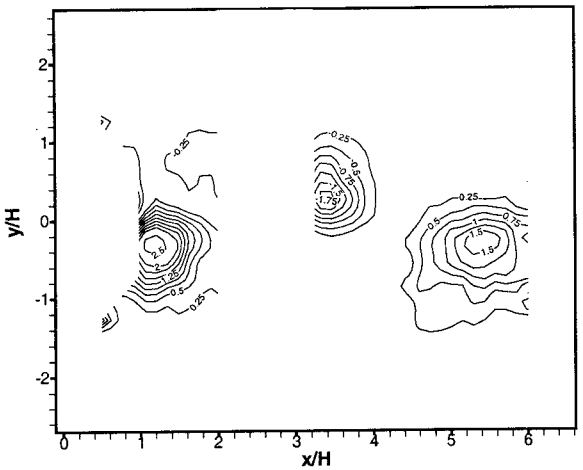

Figure 7. Phase averaged vorticity, $\omega_z/(U_o/d)$. The cylinder position is at the centreline (y ~ 0.0) and is moving downwards.

SURFACE PRESSURES

As implied by Figure 2, the spanwise correlation of surface pressures (and velocity fluctuations in the wake) increase substantially during lock-in (e.g., Sarpkaya, 1979). Figure 8, which shows segments of the pressure fluctuation time series at θ = 90° on the cylinder surface. The overall two-dimensionality is remarkable given the high Reynolds number of the flow. The Reynolds number is such that the separated shear layers should be turbulent already at the shoulder of the cylinder. This is consistent with the spanwise correlations reported in many other oscillating cylinder experiments. Thus, the shedding is significantly more two-dimensional than for stationary cylinders (cf., Figure 1) which should result in less phase jitter and less variation in the strength of the shed vortices. Bailey et al. (2002), studying a square cylinder near a wall, observed the disappearance of oblique shedding and dislocations for particular gap heights and the shedding became "tuned" as a result (see their Figures 5 and 13). Thus, it appears that the

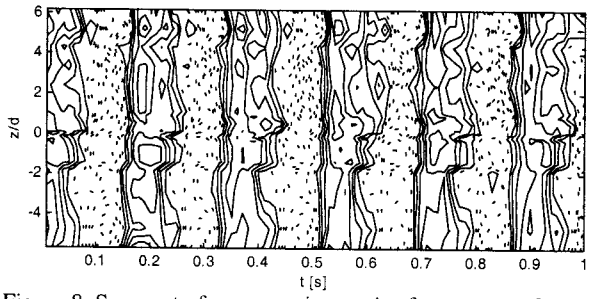

Figure 8. Segment of pressure time series from a row of taps on along the span of the cylinder.

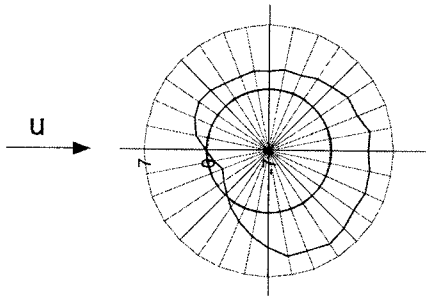

Figure 9. Phase-averaged surface pressures when the cylinder is in its uppermost position (y/D = 0.6). The plot is of suctions (Fathi, 2001).

Figure 9 shows the phase-averaged pressure (suction) distribution with the cylinder at its uppermost point. The stagnation point has moved about 20° below the centreline, but, inspite of this, the overall lift force is downwards, consistent with the numerical data presented in Sarpkaya (1979). It is difficult to assess the location of separation points from surface pressure data, but Sarpkaya points out that they move during the cycle such that when the cylinder is at its uppermost point, the lower shear layer's separation point moves further back. For stationary cylinders this would be associated with a thinner wake and reduced drag. Obviously, it is well documented that drag is not reduced for oscillating cylinders; however, the present wake does become thinner when compared to the stationary wake of CC83. This will be examined below.

INCOHERENT STRESSES AND THE PRODUCTION OF INCOHERENT TURBULENCE

Figures 10 and 11 show the phase-averaged coherent and incoherent lateral normal stresses, respectively. These illustrate an overall similarity with those from the stationary cylinder of CC83, but two particular observations can be made. Firstly, both the coherent and incoherent stresses are larger than for the stationary cylinder, consistent with both the stronger main (Karman) vortices and the resultingly stronger secondary structures, the ribs.

Secondly, and somewhat suprisingly, the wake is significantly thinner than Cantwell and Coles' wake. As discussed earlier, the vortex spacing is similar because the timing of the shedding is such that the vortices are shed near the wake centreline. Since the vortices are less three-dimensional, irregular wake thicknesses due to dislocations and bending of the Karman vortices are minimized.

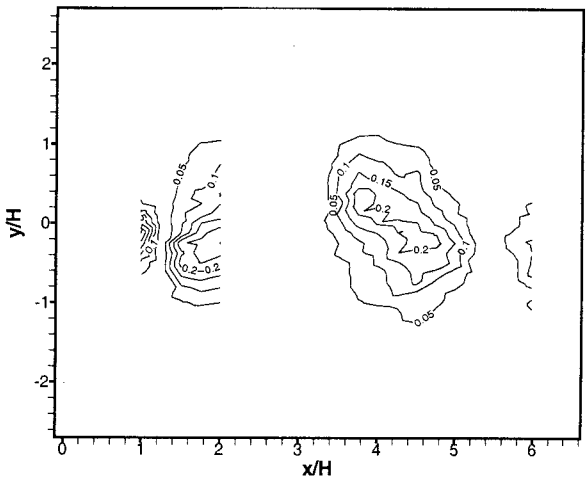

Figure 10. Phase-averaged, coherent, lateral normal stress, $\langle v_c \rangle \langle v_c \rangle$. The cylinder position is at the centreline (y ~ 0.0) and is moving downwards.

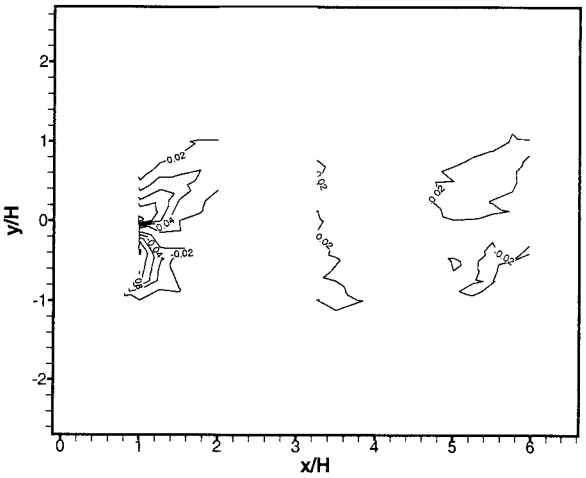

Figure 11. Phase-averaged, incoherent, lateral normal stress, $\langle v_r v_r \rangle$. The cylinder position is at the centreline (y ~ 0.0) and is moving downwards.

Figure 12 shows the production of incoherent turbulence by the coherent motions. Consistent with the observations of the turbulence stresses discussed above, the basic features of production are similar to those observed in the stationary wake; namely, production occurs primarily in the region of the saddle points. The main difference is that the magnitude is larger.

DISCUSSION

The main (Karman) vortices are associated with the large scale engulfment of irrotational fluid from the external stream (CC83) while secondary structures with streamwise vorticity, often called ribs, are believed responsible for

making the newly engulfed fluid turbulent (Hussain and Hayakawa, 1987). This occurs in the straining region of the saddle points where the ribs are stretched, and strengthened, by the strain field. In has been speculated that the ribs act to deform the main vortices into horseshoe-like structures (see Hussain and Hayakawa's Figure 11).

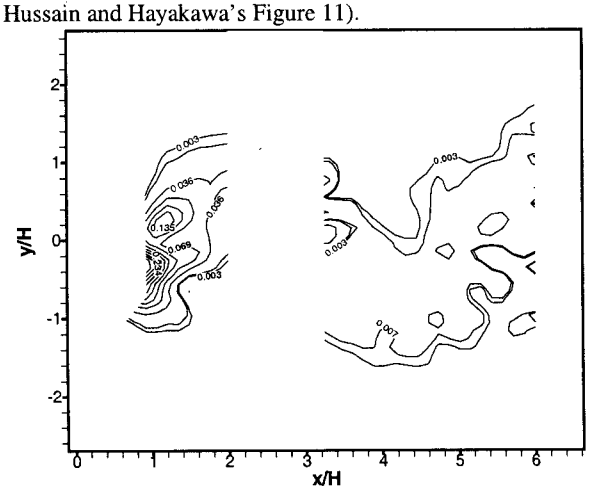

Figure 12. Phase-averaged production of incoherent stresses by the coherent motions. The cylinder position is at the centreline (y ~ 0.0) and is moving downwards.

The role the vortex dislocations play in entrainment and mixing is not currently understood, nor even how they are related to the rib structures in the base region and near wake. (At low Reynolds numbers, the ribs are associated with Type B instabilities). It is interesting that the wake of the oscillating cylinder is thinner. This could be due to (i) the greater order of the main vortices, which appears to be more significant than enhanced engulfment effected by the greater rotational speed of the vortices, or (ii) reduced engulfment because large-scale three-dimensionalities like dislocations play a significant role in near wake engulfment. In the far wake, the engulfment process is dominated by horseshoe-like vortices (Kopp et al., 2003). Perhaps the engulfment process is more complex than indicated by CC83 and Hussain and Hayakawa (1987) with dislocations enhancing the overall engulfment rates in the near field. If the ribs do indeed cause the main vortices to bend, this process would take rather longer to occur because of the greater two-dimensionality in the oscillating wake.

CONCLUSIONS

The phase-averaged velocity field of a freely vibrating circular cylinder with peak displacements (relative to the rest position) of 0.75 d was examined. It was found that the resulting velocity field was remarkably similar to that for a stationary circular cylinder in some ways, and quite different in others. Differences were attributed to the greater two-dimensionality of the vortex formation process for the oscillating cylinder.

REFERENCES

Bailey, S.C.C., Martinuzzi, R.J. & Kopp, G.A., 2002, "The effects of wall proximity on vortex shedding from a square cylinder: Three-dimensional effects," *Phys. Fluids*, vol. 14, pp. 4160-4177.

Bearman, P. W., 1984, "Vortex shedding from oscillating bluff bodies," *Ann. Rev. Fluid Mech.*, vol. 16, pp. 195-222.

Bearman, P.W. & Obasaju, E.D., 1982, "An experimental study of pressure fluctuations on fixed and oscillating square cylinder sections," *J. Fluid Mech.*, vol. 119, pp. 297-321.

Cantwell, B. & Coles, D., 1983, "An experimental study of entrainment and transport in the turbulent near wake of a circular cylinder," *J. Fluid Mech.*, vol. 136, pp. 321-374.

Davies, M.E., 1976, "A comparison of the wake structure of a stationary and oscillating bluff body using a conditional averaging technique," *J. Fluid Mech.*, vol. 75, pp. 209-231.

Eisenlohr, H. & Eckelmann, H., 1989, "Vortex splitting and its consequences in the vortex street wake of cylinders at low Reynolds numbers," *Phys. Fluids A*, vol. 1, pp. 189-192.

Fathi, S., 2001, Ph.D. Thesis, Università degli Studi "G. d'Annunzio" di Chieti-Pescara (in Italian).

Govardhan, R. & Williamson, C.H.K., 2000, "Modes of vortex formation and frequency response of a freely vibrating cylinder," *J. Fluid Mech.*, vol. 420, pp. 85-130.

Gu, W., Chyu, C. & Rockwell, D., 1994, "Timing of vortex formation from an oscillating cylinder," *Phys. Fluids*, vol. 6, pp. 3677-3682.

Havel, B., 1999, "Experimental investigation of the turbulent flow generated by two interfering surface-mounted cubes in a thin boundary layer, M.E.Sc. Thesis, University of Western Ontario.

Hussain, A.K.M.F. & Hayakawa, M., 1987, "Eduction of large-scale organized structures in a turbulent plane wake," *J. Fluid Mech.*, vol. 180, pp. 193-229.

Kamprath, M., 2001, "A report on the velocity field behind an elastically mounted circular cylinder at lock-in," Boundary Layer Wind Tunnel Laboratory Report BLWT-1-2001, University of Western Ontario.

Kopp, G.A., Giralt, F. & Keffer, J.F., 2002, "Entrainment vortices and interfacial intermittent turbulent bulges in a plane turbulent wake," *J. Fluid Mech.*, vol. 469, pp. 49-70.

Roshko, A., 1954, "On the drag and shedding frequency of two-dimensional bluff bodies," NACA Tech. Note No. 3169.

Sarpkaya, T., 1979, "Vortex-induced oscillations," *ASME J. App. Mech.*, vol. 46, pp. 241-258.

Tombazis, N. & Bearman, P.W., 1997, "A study of three-dimensional aspects of vortex shedding from a bluff body with a mild geometric disturbance," *J. Fluid Mech.*, vol. 330, pp. 85-112.

Williamson, C.H.K. & Roshko, A., 1988, "Vortex formation in the wake of an oscillating cylinder," *J. Fluids Struct.*, vol. 2, pp. 355-381.

Williamson, C.H.K., 1996, "Vortex dynamics in the cylinder wake," *Ann. Rev. Fluid Mech.*, vol. 28, pp. 477-539.